

Contrast Similarity-Aware Dual-Pathway Mamba for Multivariate Time Series Node Classification

Mingsen Du^a, Meng Chen^a, Yongjian Li^a, Xiuxin Zhang^a, Jiahui Gao^a, Cun Ji^{b,*}, Shoushui Wei^{a,*}

^a*School of Control Science and Engineering, Shandong University, Jinan, China*

^b*School of Information Science and Engineering, Shandong Normal University, Jinan, China*

Abstract

Multivariate time series (MTS) data is generated through multiple sensors across various domains such as engineering application, health monitoring, and the internet of things, characterized by its temporal changes and high dimensional characteristics. Over the past few years, many studies have explored the long-range dependencies and similarities in MTS. However, long-range dependencies are difficult to model due to their temporal changes and high dimensionality makes it difficult to obtain similarities effectively and efficiently. Thus, to address these issues, we propose contrast similarity-aware dual-pathway Mamba for MTS node classification (CS-DPMamba). Firstly, to obtain the dynamic similarity of each sample, we initially use temporal contrast learning module to acquire MTS representations. And then we construct a similarity matrix between MTS representations using Fast Dynamic Time Warping (FastDTW). Secondly, we apply the DPMamba to consider the bidirectional nature of MTS, allowing us to better capture long-range and short-range dependencies within the data. Finally, we utilize the Kolmogorov-Arnold Network enhanced Graph Isomorphism Network to complete the information interaction in the matrix and MTS node classification task. By comprehensively considering the long-range dependencies and dynamic similarity features, we achieved precise MTS node classi-

*Corresponding author

Email addresses: mingsendu@mail.sdu.edu.cn (Mingsen Du),
chchenmeng@gmail.com (Meng Chen), lyj4072021@163.com (Yongjian Li),
xiuxinzhang@mail.sdu.edu.cn (Xiuxin Zhang), gaojiahui@mail.sdu.edu.cn (Jiahui Gao),
jicun@sdu.edu.cn (Cun Ji), sswei@sdu.edu.cn (Shoushui Wei)

Preprint submitted to Engineering Applications of Artificial Intelligence November 20, 2024

fication. We conducted experiments on multiple University of East Anglia (UEA) MTS datasets, which encompass diverse application scenarios. Our results demonstrate the superiority of our method through both supervised and semi-supervised experiments on the MTS classification task.

Keywords: Multivariate Time Series Classification, Time Series Similarity, Mamba, Representation Learning, Graph Neural Network

1. Introduction

In recent years, significant advancements have been made in the field of time series analysis, driven by the growing availability of complex high-dimensional data from various sources such as sensor networks [1], financial markets [2], and biomedical applications [3]. Accurately capturing and analyzing these time series data is crucial for applications such as activity recognition [4], anomaly detection [5], and predictive modeling [6].

Among them, MTS classification is a significant research topic with applications in various fields, such as human activity recognition [4], leading to numerous studies in recent years [7, 8]. The focus of attention has been on the **similarities and long-range dependencies** inherent in MTS data [9]. However, modeling MTS data presents challenges due to temporal changes that complicate the capture of long-range dependencies, as well as high dimensional characteristics that hinder the identification of similarities between samples.

To address the above two challenges, various methods have been proposed. For **similarities extraction** challenge between time series, DTW and its variants focus on measuring the dynamic similarities between time series through nonlinear alignment. While effective in capturing temporal alignment, these methods often exhibit limitations when handling high-dimensional data, particularly in terms of expensive time complexity, which is $O(mn^2)$ (Here, m is the dimension of the MTS and n is the length). This means that when processing long sequences and high-dimensional data, the computational overhead of DTW can become prohibitively large, leading to inefficiency. Consequently, numerous methods, such as indexing (Time Series Indexing) [10], sparsification [11], lower bounding [12], and constraint path [13] have been proposed to reduce complexity and improve computational efficiency. Another difficulty is how to align the temporal dynamics to obtain more accurate similarity. When using DTW to calculate high-dimensional

MTS, the dimensions are usually added together to calculate the average, thus losing various key features of each dimension.

For **long-range dependencies extraction** challenge, deep learning methods have recently made significant progress recently. Long Short-Term Memory networks (LSTM) [14] effectively capture long-term dependencies in time series. However, LSTM models may face challenges such as high computational complexity and overfitting when dealing with long time series. Another important development is the Transformer model [15, 16, 17, 18], whose self-attention mechanism makes it possible to capture global dependencies. While Transformer suffer from quadratic complexity, leading to low computational efficiency and high costs. Recently, Selective State Space Models (SSM) like Mamba [19, 20] becomes popular, which can handle long-range dependencies in sequences while maintaining near-linear complexity, have garnered widespread attention. Numerous works have emerged in the fields of time series [20] [21], images [22], graph data [23], and natural language [24]. SSM effectively capture the dynamic properties of time series using state transition equations to describe system evolution over time. Their ability to utilize hidden states allows SSMs to simultaneously capture long-range dependencies across multiple time points, making them ideal for modeling delays and memory effects in time-dependent data.

After getting similarities and long-range dependencies, to combine both is another key challenge. In recent years, Graph Neural Networks (GNN) [25, 26] have found extensive application in the field of time series analysis, particularly in handling complex dependencies within graph-structured data involving multiple time series dimensions. In time series data, GNN can combine temporal and structural features to achieve more accurate modeling and prediction. Examples include GIN [27], GCN [28], GAT [29], Spatial-Temporal GNN [30], and GraphSAGE [31]. However, many of these methods model either static [32] or dynamic dependencies [33] between dimensions. While current time series GNN are often used to obtain feature representations of time series.

Therefore, to combine similarities and long-range dependencies, each sample in the data set can be regarded as a node in the graph. The edge relationship between nodes can be modeled using similarities, and the node features can be modeled using long-range dependencies. Recently, several researches [34, 35] combine similarities based edge relationship and node features to complete node classification.

In response to the above three challenges, we propose CS-DPMamba for

MTS node classification. Firstly, to obtain the similarity of each sample in the dataset, we initially used TemCL to acquire time series representations and then constructed a similarity matrix using FastDTW. Then, we apply DPMamba model, which considers the bidirectional nature of time series, allowing us to better capture both long-range and short-range dependencies in the time series. Finally, we utilize the KAN-GIN network for MTS node classification. By comprehensively considering the long-range dependencies and dynamic similarity features, we achieve more accurate MTS node classification.

The main contributions of this study include:

1. We propose contrast similarity-aware dual-pathway Mamba for MTS node classification and conduct experiments on the UEA dataset, demonstrating the superiority.
2. We use temporal contrastive learning to acquire time series representations and then constructed a similarity matrix between representations using FastDTW, capturing the dynamic similarities of the time series.
3. We use dual-pathway Mamba to extract high-level features from bidirectional time series while effectively managing complex data, capturing both long-range and short-range dependencies.

2. Related work

2.1. Mamba-Based Methods

Mamba was proposed [19] to address weaknesses in discrete modes by setting SSM parameters as input functions, allowing the model to selectively propagate or forget information based on the current token. Mamba integrates these selective SSMs to construct a simplified end-to-end neural network architecture that does not use attention or Multi-Layer Perceptron (MLP) block. The architecture exhibits linear scalability and can handle real-world data sequences up to millions in length. Recently, many Mamba-based methods have been proposed. TSCMamba [21] introduces a novel multi-view approach that fuses frequency-domain and time-domain features using spectral features from continuous wavelet transforms. It utilizes State Space Models (SSMs) for efficient and scalable sequence modeling, incorporating a unique tango scanning scheme to enhance sequence relationship modeling. C-Mamba [36] employs a newly developed SSM to capture cross-channel

dependencies while maintaining linear complexity and preserving a global receptive field. It integrates channel mixing to enhance the training set by combining two channels, alongside a channel attention-enhanced Mamba encoder that leverages SSM to model cross-time dependencies and inter-channel correlations. FMamba [37] first extracts temporal features of input variables through an embedding layer, then calculates dependencies between input variables with a fast attention module. Finally, Mamba selectively processes the input features, and a MLP block further extracts temporal dependencies of the variables.

2.2. Graph-Based Methods

GNN [38] can effectively capture complex relationships between different dimensions in time series by representing these dimensions and their interactions through graph structures.

Recently, many GNN-based methods have been proposed. Many models overlook seasonal effects and the evolving characteristics of shapelets. Time2Graph++ [39] addresses this by introducing a time-level attention mechanism to extract time-aware shapelets. Subsequently, time series data is transformed into shapelet evolution graphs to capture evolving patterns, further enhanced by graph attention to improve shapelet evolution. Existing methods (e.g., Transformer) struggle to effectively utilize spatial correlations between variables. To address this, Graphformer [40] efficiently learns complex temporal patterns and dependencies across multiple variables. It automatically infers an implicit sparse graph structure through a graph self-attention mechanism. Current methods mainly focus on temporal consistency, neglecting the importance of spatial consistency. TS-GAC [41] aims to enhance the spatial consistency of MTS data. Specifically, it introduces graph augmentation techniques for nodes and edges to maintain the stability of sensors and their associations. Subsequently, robust sensor and global features are extracted through node- and graph-level contrast. Graph networks can only capture spatiotemporal dependencies between node pairs and cannot handle higher-order correlations in time series. DHSL [42] uses the k-nearest neighbor method to generate a dynamic hypergraph structure from time series data and optimizes the structure through a hyper graph structure learning to capture higher-order correlations. Finally, the dynamically learned hypergraph structure is applied to a spatiotemporal hyper GNN.

Recently, several research [34] treats time series as nodes in a graph, with node similarity calculated using DTW and incorporated into the GNN. Due

to the high complexity of DTW, further research [35] uses the lower bound of DTW to calculate similarity, reducing the time complexity. However, the lower bound provides only an estimate, not an exact distance. This means that in some cases, the final similarity measure may not be accurate enough, especially in applications requiring high precision.

3. Methods

3.1. CS-DPMamba Overview

The overview involves the following steps, as shown in Fig. 1. The batch training with negative sampling is shown in Algorithm 1.

- Compute similarity matrix through ContrastFastDTW (in Section 3.2, Step 1 in Algorithm 1): Use the TemCL module to get time series representations and FastDTW to compute the similarity matrix between representations based on the sampled time-series.
- Extract long-range dependencies through DPMamba (in Section 3.3, Step 2 in Algorithm 1): Apply the DPMamba method to extract long-range dependencies from the MTS data. This step captures the relationships between different time-series data points.
- Perform node classification (in Section 3.4, Step 3 in Algorithm 1): Use the KAN-GIN to perform node classification based on long-range dependencies features and similarity matrix.
- Model update (Step 4 in Algorithm 1): Finally, update the model parameters using the processed batch to improve the model’s accuracy over multiple iterations.

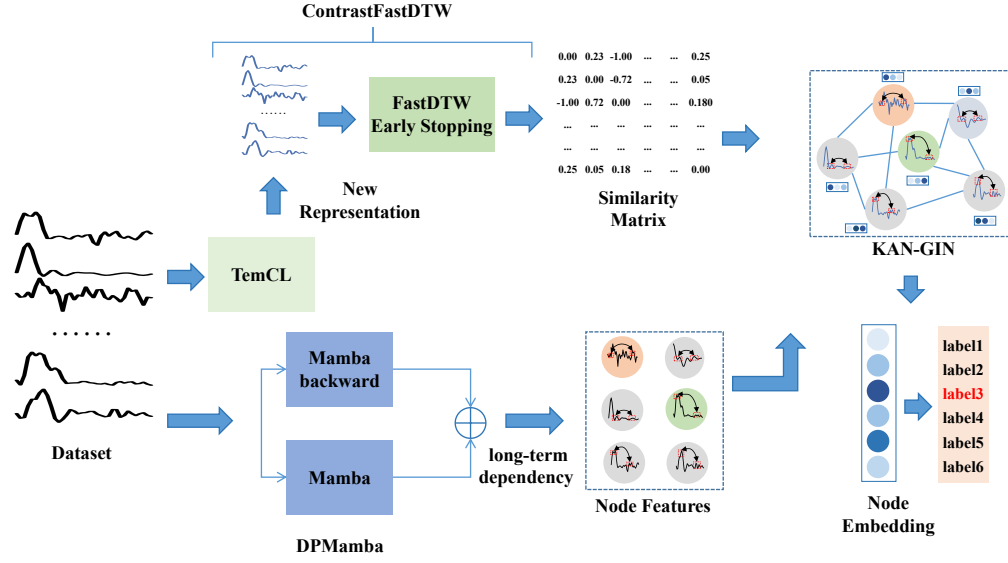


Figure 1: Overview of CS-DPMamba.

Algorithm 1 Batch Training with Negative Sampling

Require: MTS dataset, B : Batch size, E : Number of epochs, $X_{unlabeled}$: Unlabeled time series dataset, $X_{labeled}$: Labeled time series dataset, X_B : Time series of current batch

similarity_matrix \leftarrow CONTRASTFASTDTW(dataset) \triangleright Step 1: Obtain similarity matrix by Algorithm 2

for each epoch from 1 to E **do**

for each training iteration **do**

 Sample $B/2$ labeled time series from $X_{labeled}$ \triangleright Supervised training: Sample from labeled data

 Sample $B/2$ unlabeled time series from $X_{unlabeled}$ \triangleright Semi-supervised training: Sample from unlabeled data

 Construct a graph using the X_B and get $topk$ neighbors \triangleright Create a graph for current batch

 temporal_features \leftarrow DPMAMBA(X_B) \triangleright Step 2: Extract node features

 prediction \leftarrow KAN-GIN(similarity_matrix, node features) \triangleright Step 3: Execute node classification

 Update the model parameters \triangleright Use the batch to update the model \triangleright Step 4: Parameters update

end for

end for

return prediction

3.2. ContrastFastDTW based Similarity Matrix Constructing

First, to correctly align temporal dynamics and obtain more accurate similarity, we use TemCL module to obtain MTS representations (as shown in Fig. 2). And then, to obtain similarity more efficiently, we construct a similarity matrix between MTS representations using FastDTW, capturing the dynamic similarities of time series.

The similarity matrix is computed according to the following steps, detailed as shown in Algorithm 2 and Algorithm 3.

- Obtain MTS Representations (step 1 in Algorithm 2): Use temporal contrastive learning to obtain representations of the time series data. This step captures the essential features of the time series.

- Clustering (step 2 in Algorithm 2): Apply KNN clustering algorithm to get clusters based on the number of classes.
- Compute similarities within clusters (Algorithm 3 and step 3 in Algorithm 2): Calculate the distance between the representations of the MTS using FastDTWx. If they are not in the same cluster, they are considered dissimilar and a value of -1 is assigned.

3.2.1. *TemCL*

We design temporal contrast learning module (TemCL) by leveraging self-supervised learning techniques, enhances the model’s robustness to variations and noise in the time series, improves generalization performance by learning meaningful representations that can be used across different tasks. The TemCL model architecture is shown in Fig. 2. We extract temporal features by stacking multiple layers of convolution, ReLU, and max pooling modules, and construct negative samples by adding noise and cutting time series.

TemCL module has the following advantages. First, the convolutional layer can effectively extract key features in the time series through the local receptive field mechanism. This feature extraction method can capture short-term and long-term pattern changes. Second, the pooling layer reduces the dimension of the data by downsampling, thereby reducing the computational complexity. Finally, the convolutional pooling structure is robust to noise and interference. Therefore, TemCL makes the similarity measurement more accurate by optimizing the feature representation.

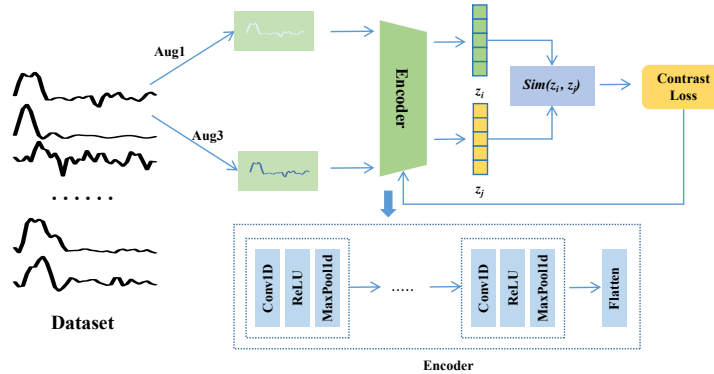


Figure 2: Contrast learning model.

Algorithm 2 ContrastFastDTW Matrix

Require: Dataset list: \mathcal{D} , target dimension: d_{target} , number of epochs: E , batch size: B , the number of class: $class$

- 1: **for** each dataset $D \in \mathcal{D}$ **do**
- 2: **if** pre-trained model exists **then**
- 3: Load pre-trained model M \triangleright Load existing pre-trained model
- 4: **else**
- 5: $M \leftarrow \text{CONTRASTLEARNING}(D)$
- 6: Train M with data D using contrastive loss \mathcal{L} \triangleright Step 1: Train model using contrastive loss
- 7: **end if**
- 8: Transform data $D \rightarrow \hat{D}$ by passing it through model M \triangleright Get representations through the model
- 9: $C_k \leftarrow \text{KNN_CLUSTER}(\hat{D}, class)$ \triangleright Step 2: Use KNN clustering to get clusters if using early stopping
- 10: $\text{DTWmatrix} \leftarrow \text{FASTDTWx}(\hat{D}, C_k)$ \triangleright Step 3: Compute the DTW matrix by Algorithm 3
- 11: **end for**
- 12: **function** CONTRASTLEARNING(D, E, B)
- 13: Initialize model M
- 14: **for** epoch $e \in \{1, \dots, E\}$ **do**
- 15: **for** batch $b \in \{1, \dots, B\}$ **do**
- 16: Get positive samples D_p from batch b
- 17: Generate negative samples $X_n \leftarrow \text{GENERATE_NEGATIVE_SAMPLES}(D_p)$ \triangleright Generate negative samples from positive samples
- 18: Define labels y with $y_i \leftarrow 1$ for positive pairs, $y_i \leftarrow 0$ for negative pairs \triangleright Label positive and negative pairs
- 19: Forward pass: $Z_p \leftarrow M(D_p), Z_n \leftarrow M(X_n)$ \triangleright Compute representations for positive and negative samples
- 20: Compute loss $\mathcal{L} \leftarrow (1 - y) \cdot \|Z_p - Z_n\|^2 + y \cdot \max(m - \|Z_p - Z_n\|, 0)^2$ \triangleright Calculate contrastive loss
- 21: **end for**
- 22: **end for**
- 23: Return M \triangleright Return the trained model
- 24: **end function**

Algorithm 3 FastDTWx

```
1: function FASTDTWx(representations= $\hat{D}$ , clusters= $C_k$ , radius=1,
  dist=Euclidean)
2:   similarity_matrix  $\leftarrow$  zeros(N, N)  $\triangleright$  Initialize similarity matrix
3:   for each cluster  $C_k$  in classes do
4:     for each sample  $i \in C_k$  do
5:       for each sample  $j \in C_k$  do  $\triangleright$  Only compute within the cluster
6:         distance  $\leftarrow$  FASTDTW(dataset[i], dataset[j], radius, dist)
 $\triangleright$  Compute similarity between samples
7:         similarity_matrix[i][j]  $\leftarrow$  distance
8:       end for
9:     end for
10:  end for
11:  for each sample  $i$  not in any cluster do
12:    for each sample  $j$  in all other clusters do
13:      similarity_matrix[i][j]  $\leftarrow$  -1  $\triangleright$  Assign dissimilarity if not in
the same cluster
14:    end for
15:  end for
16:  return similarity_matrix  $\triangleright$  Return similarity matrix
17: end function
18: function FASTDTW(x, y, radius, dist)
19:   if length of x or y  $\leq$  (radius + 2) then
20:     return DTW(x, y, dist)
21:   end if
22:   x_shrunked, y_shrunked  $\leftarrow$  REDUCEBYHALF(x), REDUCEBYHALF(y)
23:   distance, path  $\leftarrow$  FASTDTW(x_shrunked, y_shrunked, radius, dist)
24:   return distance
25: end function
```

The contrastive loss can be defined as Eq. 1.

$$\begin{aligned}\mathcal{L} = & \frac{1}{N} \sum_{i=1}^N (y_i \cdot d(f_{\text{ReLU}}(p(\text{Conv}(\mathbf{x}_i))), p(\text{Conv}(\mathbf{x}_j))))^2 \\ & + \frac{1}{N} \sum_{i=1}^N ((1 - y_i) \cdot \max(0, m - d(f_{\text{ReLU}}(p(\text{Conv}(\mathbf{x}_i))), p(\text{Conv}(\mathbf{x}_j))))^2\end{aligned}\quad (1)$$

In Eq. 1, N : Total number of training pairs. y_i : Binary label indicating similarity ($y_i = 1$) or dissimilarity ($y_i = 0$) of pair (x_i, x_j) . $d(f(x_i), f(x_j))$: Distance metric between feature representations of x_i and x_j . m : Margin defining the minimum distance between dissimilar pairs. The function f_{ReLU} includes convolution (Conv), pooling (p), and ReLU activation. By optimizing this loss function, we effectively learn representations of time series.

For generating negative samples $\mathcal{X}_{\text{negative}}$ of time series as Eq. 2 - Eq. 3.

$$\mathcal{X}_{\text{negative}} = \{\mathbf{x}'_i = \mathbf{x}_i + \mathbf{n}_i \mid \mathbf{n}_i \sim \mathcal{N}(0, \sigma^2), i = 1, 2, \dots, N\} \quad (2)$$

In Eq. 2, \mathbf{x}_i : Positive samples. \mathbf{n}_i : Noise generated from a Gaussian distribution with mean 0 and variance σ^2 .

$$\mathcal{X}_{\text{negative}} = \{\mathbf{x}'_i = \mathbf{x}_i[t_1 : t_2] \mid t_1, t_2 \text{ are non-overlapping}, i = 1, 2, \dots, N\} \quad (3)$$

In Eq. 3, \mathbf{x}'_i : Generated negative sample from positive sample \mathbf{x}_i . t_1, t_2 : Start and end indices of the time window (non-overlapping). i : Index of positive samples, where $i = 1, 2, \dots, N$.

3.2.2. Pairwise Distance Matrix for MTS

DTW is an algorithm used to measure the similarity between two time series signals. It allows for nonlinear time alignment, enabling the optimal matching of sequences even when they differ in speed or have temporal discrepancies. The DTW calculation follows the following steps:

a) DTW Formulation

Given two time series $X = (x_1, x_2, \dots, x_n)$ and $Y = (y_1, y_2, \dots, y_m)$, where x_i and y_j are elements of the series, DTW aims to find a nonlinear alignment that minimizes the alignment cost.

b) *Distance Matrix Calculation*

First, compute the distance matrix D as Eq. (4), where each element $D(i, j)$ represents the distance between the i -th element of X and the j -th element of Y . In Eq. (4), $\text{dist}(x_i, y_j)$ is typically the Euclidean distance or another distance metric.

$$D(i, j) = \text{dist}(x_i, y_j) \quad (4)$$

c) *Recursive Computation*

The distance $\text{DTW}(X, Y)$ is then recursively calculated using dynamic programming as Eq. (5). Define the cumulative distance matrix C , where $C(i, j)$ represents the minimum cumulative distance from the start point $(1, 1)$ to (i, j) .

$$C(i, j) = \text{dist}(x_i, y_j) + \min \begin{cases} C(i-1, j), & \text{(vertical move)} \\ C(i, j-1), & \text{(horizontal move)} \\ C(i-1, j-1) & \text{(diagonal move)} \end{cases} \quad (5)$$

The initial condition is Eq. (6). The final DTW distance is $C(n, m)$, representing the minimum cumulative distance from the start of series X to the end of series Y .

$$C(1, 1) = \text{dist}(x_1, y_1) \quad (6)$$

d) *FastDTW*

FastDTW [13] is an efficient algorithm for computing time series similarity, reducing the traditional $O(N^2)$ complexity of DTW to $O(N)$ through a multiresolution approximation.

3.2.3. FastDTW based Matrix

Let $\mathbf{X} = \{\mathbf{x}_1, \mathbf{x}_2, \dots, \mathbf{x}_N\}$ be a dataset of N MTS, where each $\mathbf{x}_i \in \mathbb{R}^{T \times N}$ represents a time series with T time steps and N features. The FastDTW distance between \mathbf{x}_i and \mathbf{x}_j is denoted as $\text{FastDTW}(\mathbf{x}_i, \mathbf{x}_j)$. We define the pairwise distance matrix $\mathbf{D} \in \mathbb{R}^{N \times N}$ as Eq. 7.

$$\mathbf{D}_{ij} = \text{FastDTW}(\mathbf{x}_i, \mathbf{x}_j), \quad \text{for } i, j = 1, 2, \dots, N \quad (7)$$

The matrix \mathbf{D} is a symmetric matrix where each entry \mathbf{D}_{ij} represents the FastDTW distance between time series \mathbf{x}_i and \mathbf{x}_j as Eq. 8.

$$\mathbf{D} = \begin{pmatrix} 0 & \text{FastDTW}(\mathbf{x}_1, \mathbf{x}_2) & \dots & \text{FastDTW}(\mathbf{x}_1, \mathbf{x}_N) \\ \text{FastDTW}(\mathbf{x}_2, \mathbf{x}_1) & 0 & \dots & \text{FastDTW}(\mathbf{x}_2, \mathbf{x}_N) \\ \vdots & \vdots & \ddots & \vdots \\ \text{FastDTW}(\mathbf{x}_N, \mathbf{x}_1) & \text{FastDTW}(\mathbf{x}_N, \mathbf{x}_2) & \dots & 0 \end{pmatrix} \quad (8)$$

In Eq. 8, \mathbf{D}_{ij} is the FastDTW distance between time series \mathbf{x}_i and \mathbf{x}_j . If $i = j$, $\mathbf{D}_{ii} = 0$, since the distance between a time series and itself is zero. \mathbf{D} : A symmetric matrix where $\mathbf{D}_{ij} = \mathbf{D}_{ji}$, representing all pairwise FastDTW distances among the time series in the dataset.

3.2.4. Final Similarity Matrix

After getting the FastDTW matrix D , to further describe the similarity, we perform the following processing. First, we introduce a scaling hyperparameter $\alpha \in [0, \infty)$ to control the importance of top neighbors. Specifically, let D_{ij} denote the (i, j) entry of D . The adjacency matrix A is obtained by the following formula as Eq. 9.

$$A_{ij} = \frac{1}{e^{\alpha D_{ij}}}, \quad \forall i, j \quad (9)$$

where A_{ij} represents the (i, j) entry of A . A larger α will give more importance to the top neighbors.

Next, to filter out irrelevant neighbors, we sample the top K neighbors for each node. Specifically, for each row a_i in A , we keep only the K entries with the largest weights and set the others to zero, resulting in a sparse matrix.

When handling similarity, we define a similarity function as Eq. 10.

$$\text{similarity}_{ij} = \begin{cases} 1 & \text{if } A_{ij} = 0 \\ \frac{1}{1+|A_{ij}|} & \text{if } A_{ij} > 0 \\ 0 & \text{if } A_{ij} < 0 \end{cases} \quad (10)$$

When $A_{ij} = 0$, the similarity is 1, indicating maximum similarity. When $A_{ij} > 0$, the value is calculated using $\frac{1}{1+|A_{ij}|}$, which means that when A_{ij}

is close to 0, similarity approaches 1, while larger values of A_{ij} will lead to similarity approaching 0. When $A_{ij} < 0$, the similarity is directly set to 0, indicating complete dissimilarity.

Finally, we normalize the adjacency matrix using the following formula as Eq. 11.

$$\tilde{A}_{ij} = \frac{A_{ij}}{\sum_{j'} A_{ij'}}, \quad \forall i, j \quad (11)$$

In the context of a GNN for node classification, Each MTS \mathbf{x}_i is represented as a node in a graph. The matrix \mathbf{D} defines the edge weights between nodes, where a smaller DTW distance indicates a stronger similarity and thus a stronger edge connection between nodes i and j . The GNN can use this matrix as input to perform node classification based on the structural properties of the graph formed by these time series.

3.3. Dual-Pathway Processing Using Mamba Model

We apply the dual-pathway Mamba (DPMamba, as shown in Algorithm. 4 and Fig. 3) to consider the bidirectional nature of MTS, allowing us to better capture long-range and short-range dependencies.

DPMamba captures temporal dependencies in both forward and backward directions, providing a more comprehensive modeling of time series data. The combined output from both directions can improve the accuracy of predictions, especially in cases where future data points influence past states.

3.3.1. State Evolution in Forward Direction

Given a MTS $\mathbf{x}(t)$ as input, the continuous-time state evolution is described as Eq. (12).

$$\mathbf{h}'(t) = A\mathbf{h}(t) + B\mathbf{x}(t), \quad \mathbf{y}(t) = C\mathbf{h}(t) \quad (12)$$

where $\mathbf{h}(t)$ represents the hidden state at time t , $\mathbf{x}(t)$ is the input vector at time t , A is the state transition matrix, B maps the input $\mathbf{x}(t)$ to state updates, C maps the hidden state $\mathbf{h}(t)$ to the output $\mathbf{y}(t)$.

After discretization, the formula for the forward direction as Eq. (13).

$$\mathbf{h}_t = A\mathbf{h}_{t-1} + B\mathbf{x}_t, \quad \mathbf{y}_t = C\mathbf{h}_t \quad (13)$$

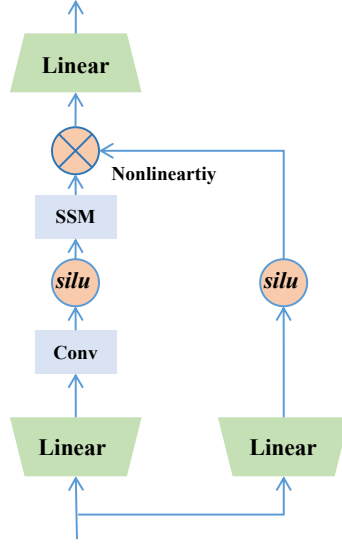


Figure 3: Structure of Mamba.

Algorithm 4 DPMamba

```

1: function DPMAMBA( $\mathbf{x}(t)$ )
2:   Initialize matrices  $A, B, C$ 
3:   Initialize hidden states  $\mathbf{h}_0$  and  $\mathbf{h}_T^R$  ▷ Forward Processing
4:   for  $t = 1$  to  $T$  do
5:      $\mathbf{h}_t \leftarrow A \cdot \mathbf{h}_{t-1} + B \cdot \mathbf{x}_t$  ▷ Update hidden state
6:      $\mathbf{y}_t \leftarrow C \cdot \mathbf{h}_t$  ▷ Compute output
7:   end for ▷ Reverse Processing
8:   for  $t = T$  down to 1 do
9:      $\mathbf{h}_t^R \leftarrow A \cdot \mathbf{h}_{t+1}^R + B \cdot \mathbf{x}_t^R$  ▷ Update reverse hidden state
10:     $\mathbf{y}_t^R \leftarrow C \cdot \mathbf{h}_t^R$  ▷ Compute reverse output
11:  end for ▷ Combine Dual-Pathway Outputs
12:  for  $t = 1$  to  $T$  do
13:     $\mathbf{y}_t^{\text{final}} \leftarrow \alpha \cdot \mathbf{y}_t + \beta \cdot \mathbf{y}_t^R$  ▷ Combine outputs
14:  end for
15:  return  $\mathbf{y}^{\text{final}}$  ▷ Return final output
16: end function

```

3.3.2. State Evolution in Reverse Direction

For reverse processing, we consider the time-reversed sequence $\mathbf{x}^R(t)$, where $\mathbf{x}^R(t) = \mathbf{x}(T - t)$. The state evolution for the reverse direction as Eq. (14). This reverse state evolution captures dependencies from future to past, complementing the forward processing.

$$\mathbf{h}_t^R = A\mathbf{h}_{t+1}^R + B\mathbf{x}_t^R, \quad \mathbf{y}_t^R = C\mathbf{h}_t^R \quad (14)$$

3.3.3. Combined Bidirectional Output

The final output is a combination of the forward and reverse outputs as Eq. (15).

$$\mathbf{y}_t^{\text{final}} = \alpha\mathbf{y}_t + \beta\mathbf{y}_t^R \quad (15)$$

where α and β are coefficients that balance the influence of forward and reverse directions, $\mathbf{y}_t^{\text{final}}$ is the final output at time t after considering both directions.

3.4. KAN-GIN Layer

We utilize the KAN to enhance the expressive power of the GIN for node classification. Although MLP are flexible in handling feature data, they fall short in capturing the complex dynamic characteristics of time series. In contrast, the KAN enhances expressive power, allowing for better integration of temporal dependencies and graph structure features in time series, thereby improving the accuracy of node classification.

After obtaining the time series similarity matrix and the node features from the Mamba model, we proceed with node classification using the KAN-GIN model. The KAN-GIN layer is defined as Eq. (16).

$$h^{(\ell)}(v) = \text{KAN}^{(\ell)} \left((1 + \epsilon) \cdot h^{(\ell-1)}(v) + \sum_{u \in \mathcal{N}(v)} h^{(\ell-1)}(u) \right) \quad (16)$$

where $h^{(\ell)}(v)$ represents the hidden state of node v at layer ℓ , $h^{(\ell-1)}(v)$ is the hidden state of node v at the previous layer $\ell - 1$, $\mathcal{N}(v)$ denotes the set of neighbors of node v , ϵ is a learnable parameter that controls the contribution of the node's own features, $\text{KAN}^{(\ell)}$ is the kernel adaptive network function applied at layer ℓ .

Table 1: 10 datasets’s description.

Abbre	Datasets	Train	Test	Dimension	Length	Classes
AF	AtrialFibrillation	15	15	2	640	3
FM	FingerMovements	316	100	28	50	2
HMD	HandMovementDirection	160	74	10	400	4
HB	Heartbeat	204	205	61	405	2
LIB	Libras	180	180	2	45	15
MI	MotorImagery	278	100	64	3000	2
NATO	NATOPS	180	180	24	51	6
PD	PenDigits	7494	3498	2	8	10
SRS2	SelfRegulationSCP2	200	180	7	1152	2
SWJ	StandWalkJump	12	15	4	2500	3

4. Experiments

4.1. Experimental Setup

4.1.1. Dataset

We selected 10 datasets from the UEA Archive [43] for our MTS classification experiments. These datasets represent the common intersection used by various comparative methods in existing study, ensuring the comparability and validity of our research. The main features and statistics of each dataset are summarized in Table. 1, covering key metrics such as the number of train and test, time series length, dimensionality, and number of classes.

We also provide supervised classification for supervised node classification, with the training and test sets as shown in the training and testing columns of Table 1. For the semi-supervised version, we randomly sample labeled instances from each class in the training data with labeled data accounted for 5%, 10%.

4.1.2. Comparison Methods

We compared 14 implementations of the following MTS classifiers, covering distance-based classifiers, state-of-the-art pattern-based models, deep learning models, and graph neural network models: ED, DTWI, DTWD (including normalized and unnormalized versions) [43]: These are commonly used distance-based models. WEASEL+MUSE [44]: An efficient time series pattern analysis toolkit. HIVE-COTE [45]: A heterogeneous ensemble classification method for time series. MLSTM-FCN [46]: A deep learning

MTS classification framework that combines LSTM layers and convolutional layers. TapNet [47]: A framework that integrates traditional methods with deep learning. MTPool [48]: Utilizes variational pooling and adaptive adjacency matrices to compute similarity using Euclidean distance. MF-Net [25]: Integrates local, global, and spatial features through graph convolution. Smate [49]: a novel semi-supervised model for learning interpretable Spatio-Temporal representations. USRL [50]: an unsupervised method for learning universal embeddings of time series, utilizing causal dilated convolutions and triplet loss with time-based negative sampling. ShapeNet [51]: a model that embeds shapelet candidates of varying lengths into a unified space using cluster-wise triplet loss. TodyNet [52]: Captures latent spatio-temporal dependencies without predefined structures, utilizing dynamic graphs and a temporal graph pooling layer. MICOS [53]: A mixed supervised contrastive learning framework that employs mixed supervised contrastive Loss to effectively leverage labels and capture complex spatio-temporal features. SVP-T [54]: Incorporates shape-level inputs to capture both temporal and variable dependencies, utilizing a variable-position encoding layer and a VP-based self-attention. DKN [55]: Combining convolutional network and transformer, while employing densely dual self-distillation for enhanced representation learning.

4.1.3. *Experimental Environment*

All models were trained in a Python 3.8 environment using PyTorch 1.10.0 with Cuda 11.3, with training lasting for 1000 epochs. The training environment was configured with the Ubuntu 20.04 operating system, equipped with an NVIDIA GeForce RTX 2080 GPU (20GB VRAM) and an Intel(R) Xeon(R) Platinum 8352V CPU (48GB RAM).

4.1.4. *Experimental Parameters*

The initial learning rate was initially set to 10^{-3} , and we used Negative Log Likelihood Loss as the loss function to optimize the model parameters. Additionally, the Adam optimizer with ReduceLROnPlateau strategy was employed for parameter updates.

The radius for FastDTW was set to 1. For the contrastive learning part, we conduct training for 500 epochs to obtain MTS representations. In the DPMamba model, we choose a single-layer structure. The KAN-GIN model was also set to both single-layer and multi-layer configurations. This design makes the model more concise and easier to train and debug, while main-

Table 2: Experiment results.

	ED	DTWI	DTWD	ED (norm)	DTWI (norm)	DTWD (norm)	WEASEL +MUSE	HIVE -COTE	MLSTM -FCN	Tap Net	MT Pool	MF -Net
AF	0.267	0.267	0.267	0.200	0.267	0.267	0.400	0.133	0.333	0.200	0.533	0.466
FM	0.519	0.513	0.529	0.510	0.520	0.530	0.550	0.550	0.580	0.470	0.620	0.620
HMD	0.279	0.297	0.231	0.278	0.297	0.231	0.365	0.446	0.527	0.338	0.486	0.445
HB	0.620	0.659	0.717	0.619	0.658	0.717	0.727	0.722	0.663	0.751	0.742	0.692
LIB	0.833	0.894	0.872	0.833	0.894	0.870	0.894	0.900	0.850	0.878	0.900	0.850
MI	0.510	0.390	0.500	0.510	0.390	0.500	0.500	0.610	0.510	0.590	0.630	0.540
NATO	0.850	0.850	0.883	0.850	0.850	0.883	0.870	0.889	0.900	0.939	0.944	0.927
PD	0.973	0.939	0.977	0.973	0.939	0.977	0.948	0.934	0.978	0.980	0.983	0.983
SRS2	0.483	0.533	0.539	0.483	0.533	0.539	0.460	0.461	0.472	0.550	0.600	0.533
SWJ	0.333	0.200	0.200	0.333	0.200	0.200	0.267	0.333	0.400	0.133	0.667	0.400
AVG	0.567	0.554	0.572	0.559	0.555	0.571	0.598	0.598	0.621	0.583	0.711	0.646
Wins	0	0	0	0	0	0	0	1	0	0	4	0

taining efficiency in feature extraction. The single-layer setup helps to avoid overfitting, especially in cases with limited data.

4.2. Experimental Analysis

This section includes both supervised (Ours) and semi-supervised (Ours 5%, Ours 10%) experiments. Table. 2 and Table. 3 present the average accuracy results of CS-DPMamba and other MTS classifiers on 10 UEA datasets. The best performances are highlighted in bold, with AVG representing the accuracy of the method across all datasets and Wins indicating the number of datasets where the best accuracy was achieved.

As shown in Table. 2 and Table. 3, CS-DPMamba outperformed other 14 state-of-the-art MTS classification methods on 4 datasets, while maintaining competitiveness across datasets with varying numbers of variables and lengths. The ranking of critical difference (CD) diagram reflects the average performance of each method across all datasets, with our method ranking second and best average accuracy (0.712), demonstrating the superiority of our approach, as shown in Fig. 4. According to the CD diagram, we can see that our semi-supervised model (Ours 5%, Ours 10%) still surpasses many methods and achieves certain results.

Our method achieved the best results on the AF, FM, and SWJ datasets, which exhibit high complexity and diversity, making them suitable for feature extraction through dynamic similarity and long-range dependencies. MT-Pool primarily utilizes Euclidean distance to calculate similarity, while our method captures dynamic similarity using FastDTW, allowing it to better

Table 3: Experiment results.

	Smate	USRL	Shape Net	DKN	Tody Net	SVP-T	MICOS	Ours	Ours (5%)	Ours (10%)
AF	0.133	0.333	0.400	0.467	0.467	0.400	0.333	0.533	0.400	0.466
FM	0.620	0.530	0.580	0.600	0.570	0.600	0.570	0.630	0.570	0.580
HMD	0.554	0.378	0.338	0.662	0.649	0.392	0.649	0.540	0.486	0.527
HB	0.741	0.751	0.338	0.765	0.756	0.790	0.766	0.742	0.692	0.722
LIB	0.849	0.850	0.856	0.900	0.850	0.883	0.889	0.894	0.850	0.856
MI	0.590	0.590	0.610	0.620	0.640	0.650	0.500	0.630	0.540	0.610
NATO	0.922	0.939	0.883	0.872	0.972	0.906	0.967	0.933	0.900	0.922
PD	0.980	0.980	0.977	0.948	0.987	0.983	0.981	0.987	0.934	0.978
SRS2	0.567	0.550	0.578	0.600	0.550	0.600	0.578	0.555	0.472	0.550
SWJ	0.533	0.400	0.533	0.533	0.467	0.467	0.533	0.667	0.467	0.467
AVG	0.649	0.630	0.609	0.697	0.691	0.667	0.677	0.712	0.631	0.690
Wins	0	0	0	3	2	3	0	4	0	0

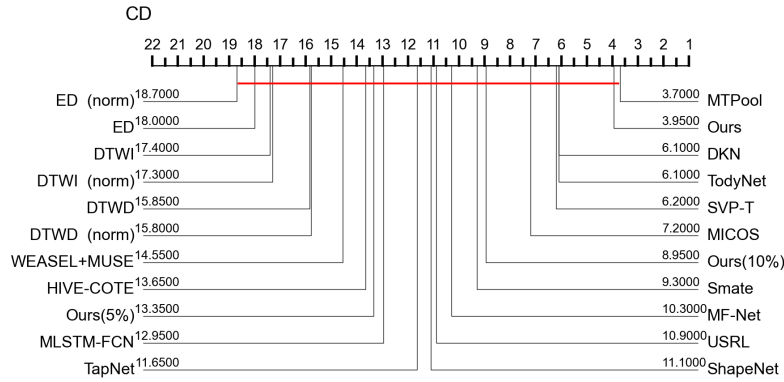


Figure 4: CD diagram.

Table 4: Representation ablation experiment results.

	Fastdtw	ContrastFastdtw
AF	0.200	0.260
FM	0.510	0.530
HMD	0.279	0.283
HB	0.692	0.697
LIB	0.305	0.333

handle the nonlinear features of time series. ShapeNet focuses on embedding shape candidates into a unified space, whereas our method demonstrates greater adaptability in similarity computation and bidirectional modeling, enabling it to handle more diverse inputs. Dyformer addresses the limitations of transformers through hierarchical pooling and adaptive learning, but our method combines graph neural networks to manage more complex structures and dynamic characteristics, achieving higher accuracy in classification tasks. TodyNet focuses on latent spatiotemporal dependencies, but our model captures richer feature relationships through similarity matrix construction and enhanced graph neural networks, improving classification results.

4.3. Ablation Study

4.3.1. Representations Ablation Experiment

We employed two methods to validate the effectiveness of the time series representations through knn: ContrastFastDTW, which combines time series representations obtained from TemCL module with FastDTW, and standard time series with FastDTW. As show in Table. 4 and Fig. 5, ContrastFastDTW achieves higher accuracy than using the original data on all datasets. The experimental results demonstrate that TemCL can effectively generate high-quality time series representations, thereby enhancing classification performance. This indicates that ContrastFastDTW is better able to capture features and patterns of representations through the strategy of contrastive learning.

4.3.2. Components Ablation Experiment

We conducted an ablation study to verify the impact of key components in CS-DPMamba on the results, specifically comparing the following models: Only DPMamba, Only KAN-GIN, Only ContrastDTW, and the complete

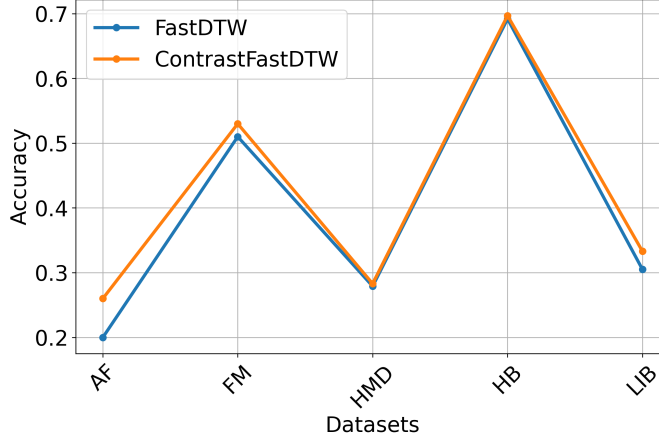


Figure 5: Representations ablation.

Table 5: Component ablation experiment results. The underlined data indicates that it ranks second.

	Only DPMamba	Only KAN-GIN	Only ContrastFastdtw	CS- DPMamba
AF	<u>0.400</u>	<u>0.400</u>	0.260	0.533
FM	0.520	<u>0.530</u>	<u>0.530</u>	0.630
HMD	0.445	<u>0.486</u>	0.283	0.540
HB	0.620	0.663	<u>0.697</u>	0.742
LIB	0.833	<u>0.850</u>	0.333	0.894

CS-DPMamba model. As shown in Table. 5 and Fig. 6, the experimental results indicate that the complete model achieves the best performance, highlighting the importance of the collaborative effect of each component on the overall performance.

4.3.3. Scale Ablation Experiment

In this section, we use different proportions (5%, 10%, 100%) of labeled data sets to conduct node classification experiments. The experimental results are shown in Table 6. We can find that as the label ratio increases, so does the accuracy.

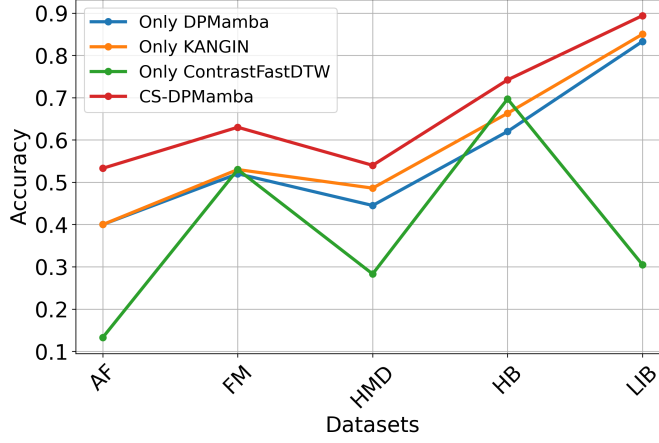


Figure 6: Component ablation.

Table 6: Using labeled data sets at different scales.

	Ours	Ours(5%)	Ours(10%)
AF	0.533	0.400	0.466
FM	0.630	0.570	0.580
HMD	0.540	0.486	0.527
HB	0.742	0.692	0.722
LIB	0.894	0.850	0.856
MI	0.630	0.540	0.610
NATO	0.933	0.900	0.922
PD	0.983	0.934	0.978
SRS2	0.555	0.472	0.550
SWJ	0.667	0.467	0.467
AVG	0.711	0.631	0.690
Wins	10	0	0

4.4. ContrastFastDTW Matrix Heatmap

Similarity matrix heatmaps (AtrialFibrillation, StandWalkJump and Hand-MovementDirection) are shown in Fig. 7. The bright grid in the figure represents a large distance (low similarity), the dark grid (high similarity), and the diagonal value is 0.

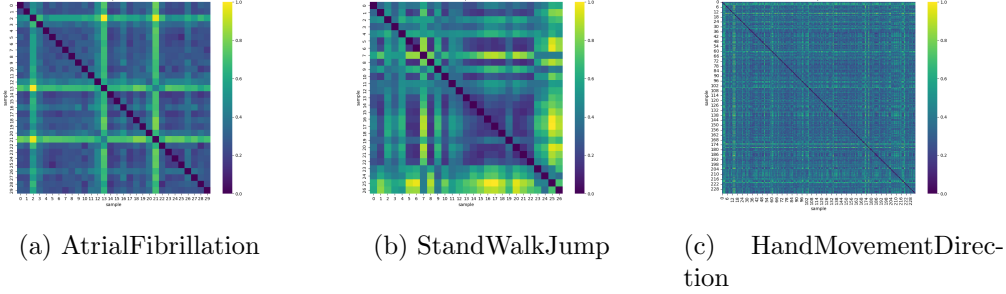


Figure 7: Comparison of Heatmaps

5. Conclusion

For the difficulty to model similarities and long-range dependencies of MTS. We propose contrast similarity-aware DPMamba for MTS node classification. First, to obtain the similarity in the dataset, we initially used TemCL to acquire time series representations and then constructed a similarity matrix between MTS samples using FastDTW, capturing the dynamic similarity characteristics of the time series. Second, we applied the DPMamba to consider the bidirectional nature of MTS, allowing us to better capture long-range and short-range dependencies within the data. Finally, we utilized the KAN to enhance the expressive power of the GIN for MTS node classification. By comprehensively considering the long-range dependencies and dynamic similarity features of time series, we achieved precise node classification. In the future, we will explore more efficient modeling methods for calculating the similarity between samples.

6. Acknowledgements

This work was supported by the National Natural Science Foundation of China [grant numbers 82072014], the National Key R&D Program of China [grant numbers 2019YFE010670], the Shandong Province Natural Science Foundation [grant numbers ZR2020MF028]. We would like to thank Eamonn Keogh and his team, Tony Bagnall and his team for the UEA/UCR time series classification repository.

7. Authors contributions

Mingsen Du: Conceptualization, Methodology, Validation, Writing–original draft, Writing–review & editing. Meng Chen: Methodology, Validation, Writing–original draft, Writing–review & editing. Yongjian Li: Methodology, Validation, Writing–original draft, Writing–review & editing. Xiuxin Zhang: Methodology, Validation, Writing–original draft, Writing–review & editing. Jiahui Gao: Methodology, Validation, Writing–original draft, Writing–review & editing. Cun Ji: Methodology, Validation, Writing–original draft, Writing–review & editing, Supervision. Shoushui Wei: Methodology, Validation, Writing–original draft, Writing–review & editing, Supervision, Project administration.

8. Data Availability

The datasets used or analyzed during the current study are available from the UEA archive: <http://timeseriesclassification.com>.

9. Code Availability

For reproducibility, we released our codes and parameters on Github: <https://github.com/dumingsen/DPMamba>.

10. Declaration of competing interest

The authors declare that they have no known competing financial interests or personal relationships that could have appeared to influence the work reported in this paper.

References

- [1] J. Wang, L. Chen, M. A. Al Faruque, Domino: Domain-invariant hyperdimensional classification for multi-sensor time series data, in: 2023 IEEE/ACM International Conference on Computer Aided Design (ICCAD), IEEE, 2023, pp. 1–9.
- [2] D. Zhan, Y. Dai, Y. Dong, J. He, Z. Wang, J. Anderson, Meta-adaptive stock movement prediction with two-stage representation learning, in: Proceedings of the 2024 SIAM International Conference on Data Mining (SDM), SIAM, 2024, pp. 508–516.

- [3] S. Yang, C. Lian, Z. Zeng, B. Xu, J. Zang, Z. Zhang, A multi-view multi-scale neural network for multi-label ecg classification, *IEEE Transactions on Emerging Topics in Computational Intelligence* 7 (3) (2023) 648–660.
- [4] P. Kumar, S. Chauhan, L. K. Awasthi, Human activity recognition (har) using deep learning: Review, methodologies, progress and future research directions, *Archives of Computational Methods in Engineering* 31 (1) (2024) 179–219. doi:0.1007/s11831-023-09986-x.
- [5] S. K. Singh, M. H. Anisi, S. Clough, T. Blyth, D. Jarchi, Cnn-bilstm based gan for anamoly detection from multivariate time series data, in: 2023 24th International Conference on Digital Signal Processing (DSP), IEEE, 2023, pp. 1–4. doi:10.1109/DSP58604.2023.10167937.
- [6] K. Yi, Q. Zhang, W. Fan, H. He, L. Hu, P. Wang, N. An, L. Cao, Z. Niu, Fouriergnn: Rethinking multivariate time series forecasting from a pure graph perspective, *Advances in Neural Information Processing Systems* 36 (2024). doi:10.48550/arXiv.2311.06190.
- [7] G. Shenderovitz, E. Sheerit, N. Nissim, Patterns of time-interval based patterns for improved multivariate time series data classification, *Engineering Applications of Artificial Intelligence* 133 (2024) 108171.
- [8] R. Lekshmi, B. R. Jose, J. Mathew, R. K. Sanodiya, Mnemonic: Multi-kernel contrastive domain adaptation for time-series classification, *Engineering Applications of Artificial Intelligence* 133 (2024) 108255.
- [9] T. M. Tran, X.-M. T. Le, H. T. Nguyen, V.-N. Huynh, A novel non-parametric method for time series classification based on k-nearest neighbors and dynamic time warping barycenter averaging, *Engineering Applications of Artificial Intelligence* 78 (2019) 173–185.
- [10] E. Keogh, C. A. Ratanamahatana, Exact indexing of dynamic time warping, *Knowledge and information systems* 7 (2005) 358–386. doi:10.1007/s10115-004-0154-9.
- [11] G. Al-Naymat, S. Chawla, J. Taheri, Sparsedtw: A novel approach to speed up dynamic time warping, *arXiv preprint arXiv:1201.2969* (2012). doi:10.48550/arXiv.1201.2969.

- [12] H. Nath, U. Baruah, Evaluation of lower bounding methods of dynamic time warping (dtw), *International Journal of Computer Applications* 94 (20) (2014) 12–17. doi:10.5120/16550-6168.
- [13] S. Salvador, P. Chan, Toward accurate dynamic time warping in linear time and space, *Intelligent Data Analysis* 11 (5) (2007) 561–580. doi:10.3233/IDA-2007-11508.
- [14] M. Beck, K. Pöppel, M. Spanring, A. Auer, O. Prudnikova, M. Kopp, G. Klambauer, J. Brandstetter, S. Hochreiter, xlstm: Extended long short-term memory, *arXiv preprint arXiv:2405.04517* (2024). doi:10.48550/arXiv.2405.04517.
- [15] N. M. Foumani, C. W. Tan, G. I. Webb, M. Salehi, Improving position encoding of transformers for multivariate time series classification, *Data Mining and Knowledge Discovery* 38 (1) (2024) 22–48. doi:10.1007/s10618-023-00948-2.
- [16] M. Cheng, Q. Liu, Z. Liu, Z. Li, Y. Luo, E. Chen, Formertime: Hierarchical multi-scale representations for multivariate time series classification, in: *Proceedings of the ACM Web Conference 2023*, 2023, pp. 1437–1445. doi:10.1145/3543507.3583205.
- [17] Y. Wu, C. Lian, Z. Zeng, B. Xu, Y. Su, An aggregated convolutional transformer based on slices and channels for multivariate time series classification, *IEEE Transactions on Emerging Topics in Computational Intelligence* 7 (3) (2022) 768–779. doi:10.1109/TETCI.2022.3210992.
- [18] J. Wen, N. Zhang, X. Lu, Z. Hu, H. Huang, Mgformer: Multi-group transformer for multivariate time series classification, *Engineering Applications of Artificial Intelligence* 133 (2024) 108633.
- [19] A. Gu, T. Dao, Mamba: Linear-time sequence modeling with selective state spaces, *arXiv preprint arXiv:2312.00752* (2023). doi:10.48550/arXiv.2312.00752.
- [20] Z. Wang, F. Kong, S. Feng, M. Wang, H. Zhao, D. Wang, Y. Zhang, Is mamba effective for time series forecasting?, *arXiv preprint arXiv:2403.11144* (2024). doi:10.48550/arXiv.2403.11144.

- [21] M. A. Ahamed, Q. Cheng, Tscmamba: Mamba meets multi-view learning for time series classification, arXiv preprint arXiv:2406.04419 (2024). doi:10.48550/arXiv.2406.04419.
- [22] L. Zhu, B. Liao, Q. Zhang, X. Wang, W. Liu, X. Wang, Vision mamba: Efficient visual representation learning with bidirectional state space model, arXiv preprint arXiv:2401.09417 (2024). doi:10.48550/arXiv.2401.09417.
- [23] R. Bresson, G. Nikolentzos, G. Panagopoulos, M. Chatzianastasis, J. Pang, M. Vazirgiannis, Kagnns: Kolmogorov-arnold networks meet graph learning, arXiv preprint arXiv:2406.18380 (2024). doi:10.48550/arXiv.2406.18380.
- [24] B. N. Patro, V. S. Agneeswaran, Mamba-360: Survey of state space models as transformer alternative for long sequence modelling: Methods, applications, and challenges, arXiv preprint arXiv:2404.16112 (2024). doi:10.48550/arXiv.2404.16112.
- [25] M. Du, Y. Wei, X. Zheng, C. Ji, Multi-feature based network for multivariate time series classification, Information Sciences 639 (2023) 119009. doi:10.1016/j.ins.2023.119009.
- [26] M. Du, Y. Wei, Y. Hu, X. Zheng, C. Ji, Multivariate time series classification based on fusion features, Expert Systems with Applications 248 (2024) 123452. doi:10.1016/j.eswa.2024.123452.
- [27] K. Xu, W. Hu, J. Leskovec, S. Jegelka, How powerful are graph neural networks?, arXiv preprint arXiv:1810.00826 (2018). doi:10.48550/arXiv.1810.00826.
- [28] T. N. Kipf, M. Welling, Semi-supervised classification with graph convolutional networks, arXiv preprint arXiv:1609.02907 (2016). doi:10.48550/arXiv.1609.02907.
- [29] X. Wang, H. Ji, C. Shi, B. Wang, Y. Ye, P. Cui, P. S. Yu, Heterogeneous graph attention network, in: The world wide web conference, 2019, pp. 2022–2032. doi:10.1145/3308558.3313562.
- [30] S. Yan, Y. Xiong, D. Lin, Spatial temporal graph convolutional networks for skeleton-based action recognition, in: Proceedings of the AAAI

- conference on artificial intelligence, Vol. 32, 2018. doi:10.1609/aaai.v32i1.12328.
- [31] W. Hamilton, Z. Ying, J. Leskovec, Inductive representation learning on large graphs, *Advances in neural information processing systems* 30 (2017). doi:10.48550/arXiv.1706.02216.
 - [32] C. Xu, F. Su, J. Lehmann, Time-aware graph neural networks for entity alignment between temporal knowledge graphs, *arXiv preprint arXiv:2203.02150* (2022). doi:10.18653/v1/2021.emnlp-main.709.
 - [33] Z. Shao, Z. Zhang, F. Wang, Y. Xu, Pre-training enhanced spatial-temporal graph neural network for multivariate time series forecasting, in: *Proceedings of the 28th ACM SIGKDD conference on knowledge discovery and data mining*, 2022, pp. 1567–1577. doi:10.1145/3534678.3539396.
 - [34] D. Zha, K.-H. Lai, K. Zhou, X. Hu, Towards similarity-aware time-series classification, in: *Proceedings of the 2022 SIAM International Conference on Data Mining (SDM)*, SIAM, 2022, pp. 199–207. doi:10.1137/1.9781611977172.23.
 - [35] W. Xi, A. Jain, L. Zhang, J. Lin, Efficient and accurate similarity-aware graph neural network for semi-supervised time series classification, in: *Pacific-Asia Conference on Knowledge Discovery and Data Mining*, Springer, 2024, pp. 276–287. doi:10.1007/978-981-97-2266-2_22.
 - [36] C. Zeng, Z. Liu, G. Zheng, L. Kong, C-mamba: Channel correlation enhanced state space models for multivariate time series forecasting, *arXiv preprint arXiv:2406.05316* (2024). doi:10.48550/arXiv.2406.05316.
 - [37] S. Ma, Y. Kang, P. Bai, Y.-B. Zhao, Fmamba: Mamba based on fast-attention for multivariate time-series forecasting, *arXiv preprint arXiv:2407.14814* (2024). doi:10.48550/arXiv.2407.14814.
 - [38] M. Jin, H. Y. Koh, Q. Wen, D. Zambon, C. Alippi, G. I. Webb, I. King, S. Pan, A survey on graph neural networks for time series: Forecasting, classification, imputation, and anomaly detection, *IEEE Transactions on Pattern Analysis and Machine Intelligence* (2024). doi:10.1109/TPAMI.2024.3443141.

- [39] Z. Cheng, Y. Yang, S. Jiang, W. Hu, Z. Ying, Z. Chai, C. Wang, Time2graph+: Bridging time series and graph representation learning via multiple attentions, *IEEE Transactions on Knowledge and Data Engineering* 35 (2) (2021) 2078–2090. doi:10.1109/TKDE.2021.3094908.
- [40] Y. Wang, H. Long, L. Zheng, J. Shang, Graphformer: Adaptive graph correlation transformer for multivariate long sequence time series forecasting, *Knowledge-Based Systems* 285 (2024) 111321. doi:10.1016/j.knosys.2023.111321.
- [41] Y. Wang, Y. Xu, J. Yang, M. Wu, X. Li, L. Xie, Z. Chen, Graph-aware contrasting for multivariate time-series classification, in: *Proceedings of the AAAI Conference on Artificial Intelligence*, Vol. 38, 2024, pp. 15725–15734. doi:10.1609/aaai.v38i14.29501.
- [42] S. Wang, Y. Zhang, X. Lin, Y. Hu, Q. Huang, B. Yin, Dynamic hyper-graph structure learning for multivariate time series forecasting, *IEEE Transactions on Big Data* (2024). doi:10.1109/TBDATA.2024.3362188.
- [43] A. Bagnall, H. A. Dau, J. Lines, M. Flynn, J. Large, A. Bostrom, P. Southam, E. Keogh, The uea multivariate time series classification archive, 2018, arXiv preprint arXiv:1811.00075 (2018).
- [44] P. Schäfer, U. Leser, Multivariate time series classification with weasel+muse, arXiv preprint arXiv:1711.11343 (2017).
- [45] A. Bagnall, M. Flynn, J. Large, J. Lines, M. Middlehurst, A tale of two toolkits, report the third: on the usage and performance of hive-cote v1.0, arXiv preprint arXiv:2004.06069 (2020).
- [46] F. Karim, S. Majumdar, H. Darabi, S. Harford, Multivariate lstm-fcns for time series classification, *Neural networks* 116 (2019) 237–245.
- [47] X. Zhang, Y. Gao, J. Lin, C.-T. Lu, Tapnet: Multivariate time series classification with attentional prototypical network, in: *Proceedings of the AAAI conference on artificial intelligence*, Vol. 34, 2020, pp. 6845–6852.
- [48] Z. Duan, H. Xu, Y. Wang, Y. Huang, A. Ren, Z. Xu, Y. Sun, W. Wang, Multivariate time-series classification with hierarchical variational graph pooling, *Neural Networks* 154 (2022) 481–490.

- [49] J. Zuo, K. Zeitouni, Y. Taher, Smate: Semi-supervised spatio-temporal representation learning on multivariate time series, in: 2021 IEEE International Conference on Data Mining (ICDM), IEEE, 2021, pp. 1565–1570.
- [50] J.-Y. Franceschi, A. Dieuleveut, M. Jaggi, Unsupervised scalable representation learning for multivariate time series, *Advances in neural information processing systems* 32 (2019).
- [51] G. Li, B. Choi, J. Xu, S. S. Bhowmick, K.-P. Chun, G. L.-H. Wong, Shapenet: A shapelet-neural network approach for multivariate time series classification, in: *Proceedings of the AAAI conference on artificial intelligence*, Vol. 35, 2021, pp. 8375–8383.
- [52] H. Liu, D. Yang, X. Liu, X. Chen, Z. Liang, H. Wang, Y. Cui, J. Gu, Todynnet: temporal dynamic graph neural network for multivariate time series classification, *Information Sciences* (2024) 120914.
- [53] S. Hao, Z. Wang, A. D. Alexander, J. Yuan, W. Zhang, Micos: Mixed supervised contrastive learning for multivariate time series classification, *Knowledge-Based Systems* 260 (2023) 110158.
- [54] R. Zuo, G. Li, B. Choi, S. S. Bhowmick, D. N.-y. Mah, G. L. Wong, Svp-t: a shape-level variable-position transformer for multivariate time series classification, in: *Proceedings of the AAAI Conference on Artificial Intelligence*, Vol. 37, 2023, pp. 11497–11505.
- [55] Z. Xiao, H. Xing, R. Qu, L. Feng, S. Luo, P. Dai, B. Zhao, Y. Dai, Densely knowledge-aware network for multivariate time series classification, *IEEE Transactions on Systems, Man, and Cybernetics: Systems* (2024).